ISSN 1392-2114 ULTRAGARSAS, Nr.1(62). 2007.

Measurement of complex impedance of ultrasonic transducers

L. Svilainis, V. Dumbrava

Signal processing department, Kaunas University o f Technology,
Studentu str. 50, LT-51368 Kaunas, Lithuania, tel. +370 37 300532, E-mail.:svilnis@ktu.lt

Abstract

The automated system for ultrasonic transducer complex impedance measurement using the sine wave correlation for signal amplitude and phase extraction is presented. The system contains the direct digital synthesis (DDS) generator and two ADC channels with a common reference frequency source. In such a case the frequency error between the excitation and the measurement channels is reduced. The shielded measurement chamber with local low noise high impedance preamplifiers has been added to reduce the induced noise and to improve robustness. The measurement procedure and equations are presented. The results of various ultrasonic transducers impedance measurements are given.

Keywords: Ultrasonic transducer impedance, data acquisition, complex impedance measurement, sine fitting, sine correlation.

Introduction

The transducer electrical impedance affects an ultrasonic transducer noise performance [1], driving response [2], bandwidth and sensitivity [3]. Having the ultrasonic transducer impedance response over the frequency band, the mentioned influence can be estimated. The complex impedance allows for even better judgment. Therefore there is a need for ultrasonic transducer complex impedance measurement. The techniques for measurement the of a transducer impedance employ an external generator and the analog-to-digit converter (ADC) for voltage and current measurements [3-5]. The technique presented is using the sine wave correlation for signal amplitude and phase extraction. The aim of investigation presented is to inspect the suitability of the designed system for ultrasonic transducer complex impedance frequency response measurements.

Measurement setup

The use of a separate generator and ADC will impose the frequency error which will have to be compensated, using the advanced fitting techniques in order to determine the frequency [6,7]. If both the generator reference frequency and the ADC reference frequency use the same source, the mentioned problems are significantly reduced. We have decided to use the complete AC parameters measurement system [8]. The system contains the direct digital synthesis (DDS) generator and two ADC channels Ch1 and Ch2 with a common reference oscillator.

The measurement system systematic error sources we are the following [5]:

- the reference impedance R_{ref};
- the ADC board input impedances;
- the acquisition channel nonlinearity;
- the parasitic impedances in grounding, shielding and cabling.

Therefore the shielded measurement chamber with local low noise high impedance preamplifiers has been added to the system to reduce the induced noise and to improve the robustness of measurements. The connections diagram and the structure of the internal measurement chamber is presented in Fig.1.

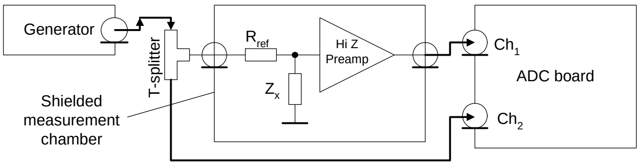

Fig. 1**. Measurement setup**

The generator output is supplied to the measurement chamber using a 50Ω RG174U cable. The coaxial T-splitter is used to route the signal to the ADC channel 2. The high impedance preamplifier output is connected to the ADC channel 1. ADC inputs and generator output have 50Ω termination impedances. Using the defined the low impedance signal path in a signal source reduces the influence of the Ch2 impedance. The high impedance preamplifier placed locally allows for a better impedance control of Ch1. The shielded case and minimized connections inside the chamber allow for reduction of grounding impedances. All the measures mentioned above allow to reduce cabling. The reference impedance R_{ref} is a high precision surface mount resistor soldered directly on the chamber PCB. The ADC nonlinearity can be evaluated using a calibration procedure. A channel is accurately characterized by using the histogram method for ADC testing [9]. A lookup table can be used to compensate the degradation on the acquisition performance with a frequency.

Closer examination of the measurement chamber connections indicate that such setup can be easily simplified to the schematic diagram presented in Fig.2.

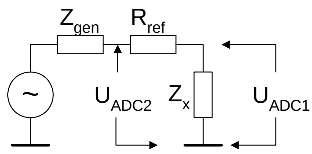

Fig. 2**. Simplified connections diagram**

The measured impedance Z_x can be calculated as:

$$\bar{Z}_x = \frac{\bar{U}_x}{\bar{I}_x}, \tag{1}$$

where U_x is the complex voltage on measured impedance taps, I_x is the complex current flowing in measured impedance. Using the notation used in Fig.2, the U_x and I_x are given by:

$$\overline{U}_x = \overline{U}_{ADC\,1};\ \overline{I}_x = \frac{\overline{U}_{ADC\,2} - \overline{U}_{ADC\,1}}{R_{ref}}, \quad (2)$$

The measurement procedure is very simple and consists of the following steps:

(i) the exciting generator is adjusted to produce a sine wave with the desired measurement frequency and amplitude;

(ii) the acquisition channels simultaneously acquire data records corresponding to the voltages U_{ADC1} and U_{ADC2};

(iii) voltages U_{ADC1} and U_{ADC2} in measurement channels introduced due to gain mismatch are measured at shorted R_{ref} and removed the Z_x condition.

(iv) voltages U_{ADC1} and U_{ADC2} due to gain mismatch are calculated and corrected for;

(v) the measured impedance Z_x is calculated:

$$\overline{Z}_x = \frac{\overline{U}_{ADC\,1}}{\overline{U}_{ADC\,2} - \overline{U}_{ADC\,1}} \cdot R_{ref}. \quad (3)$$

The main random error source is the noise present in any system. The use of sine-fitting techniques can largely reduce the influence of a noise in final results [5]. Since we use the same reference frequency for DDS used to generate the exciting signal and the acquisition ADC, the more simple form of sine-fitting can be used. Then the wave to be fit is defined as:

$$u(t) = A\cos(2\pi ft) + B\sin(2\pi ft) + C, \quad (4)$$

where A and B are the in-quadrature sine amplitudes of the sine wave, C is the DC component and f is the excitation frequency used. Fitting this function to the set of M samples, $y_1 \ldots y_M$, acquired at a frequency f_s at time instances $t_1 \ldots t_M$, is accomplished by seeking the minimum of approximation error root-mean-square (RMS) value:

$$\varepsilon_{RMS} = \sqrt{\frac{1}{M}\sum_{m=1}^{M}\left[y_m - \left[A\cos(2\pi ft_m) + B\sin(2\pi ft_m) + C\right]\right]^2}. \quad (5)$$

The procedure is simple and iterative, thus consuming a lot of a computational time. The other approach could be to use a non-iterative procedure. This requires only the construction of a M x 3 matrix and determination of its pseudo-inverse matrix and multiplication with the actual samples. The least-squares estimated parameters are obtained from

$$x = \left[D^T D\right]^{-1}\left[D^T y\right] = D^* y, \quad (6)$$

where x is the estimated parameter vector, D is the matrix that linearly relates the estimated parameters and the samples y. D^* is the Moore–Penrose pseudoinverse matrix.

Then
$$x = \begin{bmatrix} A \\ B \\ C \end{bmatrix}, \quad (7a)$$

$$D = \begin{bmatrix} w(f,t_1) & g(f,t_1) & 1 \\ w(f,t_2) & g(f,t_2) & 1 \\ \vdots & \vdots & \vdots \\ w(f,t_M) & g(f,t_M) & 1 \end{bmatrix}, \quad (7b)$$

where

$$w(f,t) = \cos(2\pi ft), \quad (7c)$$

$$g(f,t) = \sin(2\pi ft). \quad (7d)$$

The closer look at the operations performed indicate the close similarity of the operations performed to a correlation procedure, inherent in the Fourier transform. Therefore the procedure can be presented in a simplified way which is more computational efficient and is closer to programming conventions in a signal processing:

$$A = \frac{\sum_{m=1}^{M}\left[\cos(2\pi ft_m)\cdot y_m\right]}{\sum_{m=1}^{M}\left[\cos(2\pi ft_m)\right]^2}, \quad (8a)$$

$$B = \frac{\sum_{m=1}^{M}\left[\sin(2\pi ft_m)\cdot y_m\right]}{\sum_{m=1}^{M}\left[\sin(2\pi ft_m)\right]^2}, \quad (8b)$$

$$C = \frac{\sum_{m=1}^{M} y_m}{M}. \quad (8c)$$

Then the measured signal magnitude is

$$U = \sqrt{A^2 + B^2}, \quad (9a)$$

and the phase

$$\varphi = \arctan\left(\frac{B}{A}\right). \quad (9b)$$

The same computational procedure has to be performed on both ADC channels Ch1 and Ch2.

The systematic and random errors, constituting accuracy estimation of the AC parameters measurement system [8] have been investigated in [10]. The investigation included theoretical equations analysis, simulation and real system experiments. The obtained estimations of a system precision can be used in evaluating the results obtained using the forementioned acquisition system.

The measurement results

The AC parameters measurement system [8] has been used to obtain several ultrasonic transducers impedances.

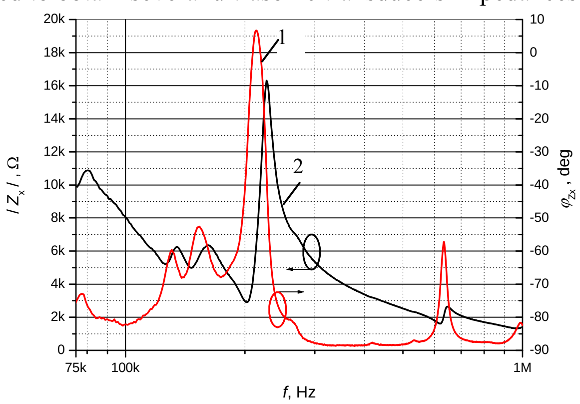

Fig. 3. **Air coupled 200 kHz transducer impedance $|Z_x|$ (1)and the phase φ_{Zx} (2) vs. frequency**

Air-coupled, 200 kHz operating frequency ultrasonic transducer impedance has been measured. The impedance magnitude $|Z_x|$ and the phase φ_{Zx} response are presented in Fig.3. The real and imaginary parts of the transducer impedance have been used to calculate the magnitude and the phase frequency response. Radial and secondary resonances are visible in the obtained impedance magnitude and phase plots in Fig.3.

It would be interesting to use the measured complex impedance to obtain the parameters of the ultrasonic transducer model. In [1] ultrasonic system noise performance has been evaluated using the Butterworth-Van Dyke (BVD) transducer model. Therefore the BVD model with 1 and 2 serial resonant tanks have been obtained, using complex impedance response fitting to the measured Z_x. The Matlab procedure *fmins*, employing the Nelder-Mead simplex method [11] have been used for fitting. Three Z_{aprox} fitting convergence rules have been used:

(i) Approximation error RMS value of the real and imaginary impedance parts:

$$\varepsilon_{\mathrm{Re}\,RMS}=\sqrt{\frac{1}{N}\sum_{n=1}^{N}\left[\mathrm{Re}\left(Z_{x,n}\right)-\mathrm{Re}\left(Z_{aprox,n}\right)\right]^2}\,, \quad (10a)$$

$$\varepsilon_{\mathrm{Im}\,RMS}=\sqrt{\frac{1}{N}\sum_{n=1}^{N}\left[\mathrm{Im}\left(Z_{x,n}\right)-\mathrm{Im}\left(Z_{aprox,n}\right)\right]^2}\,, \quad (10b)$$

$$\varepsilon_{RMS}=\varepsilon_{\mathrm{Re}\,RMS}+\varepsilon_{\mathrm{Im}\,RMS}\,; \quad (10c)$$

(ii) Approximation error RMS value of the impedance magnitude:

$$\varepsilon_{\mathrm{Re}\,RMS}=\sqrt{\frac{1}{N}\sum_{n=1}^{N}\left[\left|Z_{x,n}\right|-\left|Z_{aprox,n}\right|\right]^2}\,, \quad (11)$$

(iii) Approximation error RMS value of the impedance phase:

$$\varepsilon_{RMS}=\sqrt{\frac{1}{N}\sum_{n=1}^{N}\left[\varphi_{Z_{x,n}}-\varphi_{Z_{aprox,n}}\right]^2}\,. \quad (12)$$

Here N is the total number of impedance frequency response points, n is the point number.

The real and imaginary Z_x parts (solid lines) of the same air-coupled 200kHz transducer and their approximations using BVD model with 1 and 2 serial resonant tanks (dashed and dotted lines) are plotted in Fig.4.

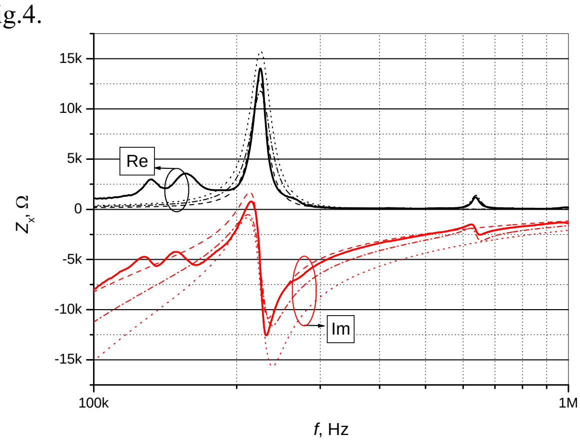

Fig. 4. **Measured impedance approximation using the BVD model**

The obtained BVD model parameters are presented in Table 1. Approximation with one serial resonant tank and using the Eq. 10 for a convergence rule is plotted by dashed lines (noted as 1STe10 in Table 1). Approximation with one serial resonant tank and using the Eq. 11 for convergence rule is noted as 1STe11 in Table 1. The one serial resonant tank and the Eq. 12 as application result of a convergence rule is plotted by dotted lines (notation 1STe12 in Table 1). Use of 2 tanks for transducer modeling and Eq. 12 as convergence rule is plotted by the dash-dot lines (2STe12 in Table 1). The results of application of Eq. 10 and Eq. 11 are very similar, as can be seen by analysis of the obtained BVD parameters in Table 1. Therefore, of Eq. 11 result of application for a convergence rule is not shown in Fig.4.

Table 1. **Transducer BVD model electrical parameters**

Parameter	1STe10	1STe11	1STe12	2STe12
C_0, pF	138.10	137.80	77.094	100.76
R_{S1},Ω	2053.7	1883.4	5331.6	3897.4
C_{S1}, pF	41.384	40.976	21.291	28.569
L_{S1},mH	15.9	15.8	29.8	22.2
R_{S2},Ω				4673.3
C_{S2}, pF				3.1175
L_{S2},mH				20.5

The presented BVD model fitting to the measured Z_x results is only the demonstration of how the measurement results can be employed further. Other models can be successfully fit into measurement results, yielding better precision. Also new mechanical or acoustical parameters can be evaluated based on a model fitting.

The impedance measurement procedure is automated and results can be obtained quickly. As a demonstration of possibilities, a PZT ceramic disk impedance frequency response has been measured while changing one surface damping conditions. The disk impedance frequency response is presented in a complex coordinate system in Fig.5 and as real and imaginary impedance parts in Fig.6.

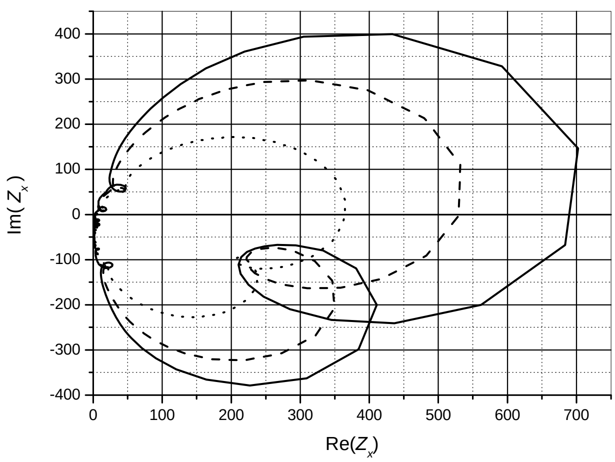

Fig. 5. **Transducer Z_x polar plot in a complex coordinate system**

The impedance frequency response of the unloaded disk was measured first (solid line). Then one disk face was loaded with a light foam damper and the impedance measured (the dashed line). The impedance measurement results obtained by loading one disk face with a high viscosity latex damper are plotted by the dotted curve. The same results are presented as real and imaginary impedance parts in Fig.6.

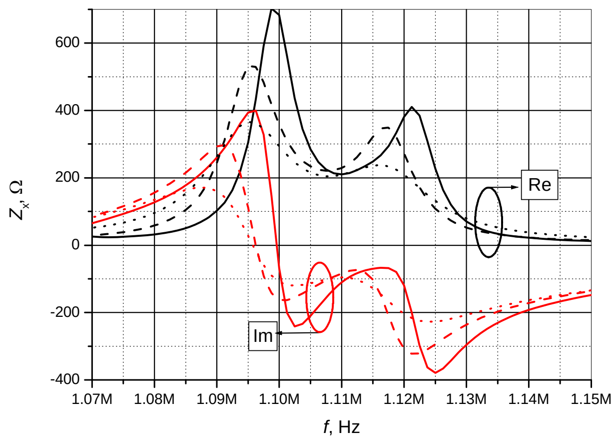

Fig. 6. **PZT disk impedance variation with damping**

Such investigation would prove useful during the design or manufacturing process of an ultrasonic transducer. The impedance can be verified after every processing stage.

The radio frequency (RF) transformers are extensively used in ultrasonic equipment [12]. By modification of source impedance the amplifier noise optimal impedance can be matched. This improves the noise performance of an ultrasonic system. The transformer also allows the effective amplifier input DC biasing thanks to a winding inductance.

If matching transformer is not properly chosen, degradation of the frequency response performance might take place. Therefore application of the matching transformer should be verified by impedance or AC response measurements. The impedance measurement results presented in Fig.7 indicate the case when a matching transformer is used.

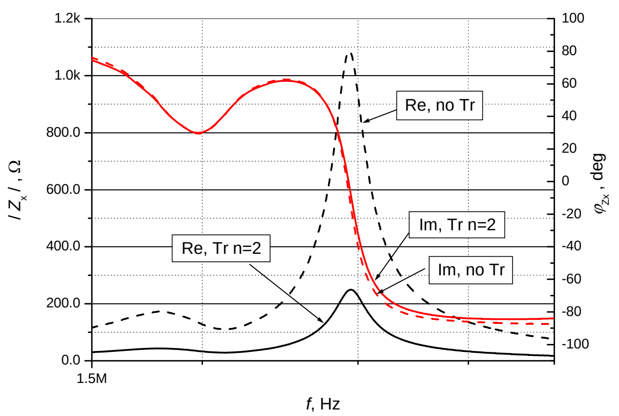

Fig. 7 **Impedance modification by matching transformer**

The phoenix SSW 70° 2MHz transducer impedance has been measured (the dashed curve). Then a matching transformer with turns ratio 2 has been added. The higher turns section has been connected to the transducer and the lower turns have been connected to the measurement system. The measurement results indicate there was no frequency response performance degradation due to implementation transformer. Note the same phase response in the matched and unmatched case.

Conclusions

The sine wave correlation for extraction of signal amplitude and phase is used. The use of the same frequency reference source for the exciting generator and the signals acquisition allows for significant simplification of a measurement procedure. The goal of the investigation presented is to indicate the multitude of applications of the obtained ultrasonic transducer complex impedance.

References

1. **Dumbrava V., Svilainis L.** Ultragarsinio keitiklio pradinio stiprintuvo triukšminis modelis. Elektronika ir elektrotechnika. Kaunas: Technologija. 2006. Nr.2(66). P. 62 – 66.
2. **Ramos A., San Emeterio J. L., Sanz P. T.** Dependence of pulser driving responses on electrical and motional characteristics of NDE ultrasonic probes. Ultrasonics. 2000. Vol.38. P.553–558.
3. **Schmerr L. W., Lopez-Sanchez A., Huang R.** Complete ultrasonic transducer characterization and its use for models and measurements. Ultrasonics. 2006. (submitted for publication)
4. **Radil T., Ramos P. M., Serra A. C.** DSP based portable impedance measurement instrument using sine-fitting algorithms, in: IMTC 2005—Instrumentation and Measurement Technology Conference, Ottawa, Canada. 2 May, 2005.
5. **Ramos P. M., Silva M. F., Serra A. C.** Low frequency impedance measurement using sine-fitting. Measurement. 2004. Vol.35. P. 89–96.
6. **Fonseca da Silva M., Serra A. C.** New methods to improve convergence of sine fitting algorithms. Computer Standards and Interfaces. 2003. P. 23–31.
7. **Ramos P. M., Fonseca da Silva M., Serra A. C.** Improving sine-ftting algorithms for amplitude and phase measurements, in: XVII IMEKO World Congress, Croatia, 2003. Vol.TC4. P. 614–619.
8. **Svilainis L.** The AC parameters measurement system for ultrasonics. Ultragarsas (Ultrasound). Kaunas: Technologija. 2006. Nr.3(60). P.44-48.
9. **Alegria F., Arpaia P., Da Serra A. M C., Daponte P.** Performance analysis of an ADC histogram test using small triangular waves, IEEE Transactions on Instrumentation and Measurements. 2002. Vol.51. P. 723–729.
10. **Svilainis L., Dumbrava V.** Amplitude and phase measurement in acquisition systems. Matavimai (Measurements), Kaunas: Technologija, 2006, *in press*.
11. **Lagarias J. C., Reeds J. A., Wright M. H., Wright P. E.** Convergence properties of the Nelder-Mead simplex method in low dimensions. SIAM J. OPTIM. 1998. Vol.9. No.1. P. 112-147.
12. **Dumbrava V., Svilainis L.** Application of transformer for improvement of noise performance of ultrasonic preamplifier. Ultragarsas (Ultrasound). Kaunas: Technologija. 2005. No.4(57). P.22-28.

L. Svilainis,V. Dumbrava

Ultragarsinių keitiklių kompleksinio impedanso matavimas

Reziumė

Aptarta automatizuotoji ultragarsinių keitiklių kompleksinio impedanso matavimo sistema. Signalo amplitudei ir fazei gauti naudojama sinusinio signalo koreliacija. Sistema sudaryta iš DDS generatoriaus ir dviejų kanalų skaitmeninio analogo keitiklio su bendru atraminio dažnio šaltiniu. Tokiu atveju dažnio paklaida tarp zondavimo ir matavimo kanalų sumažinama. Panaudota ekranuotoji matavimo kamera su didelės įėjimo varžos mažatriukšmiais pradiniais stiprintuvais. Tai leidžia sumažinti iš išorės indukuojamų signalų lygį ir padidinti matavimų stabilumą. Aptarta matavimo procedūra ir pateikiamos lygtys. Aprašyti įvairių ultragarsinių keitiklių kompleksinio impedanso matavimo rezultatai.

Pateikta spaudai 2006 11 21